

JPRS-JST-90-007
31 JANUARY 1990



**FOREIGN
BROADCAST
INFORMATION
SERVICE**

JPRS Report

Science & Technology

***Japan
18th FRP Symposium***

19980129 100

REPRODUCED BY
U.S. DEPARTMENT OF COMMERCE
NATIONAL TECHNICAL INFORMATION SERVICE
SPRINGFIELD, VA. 22161

DTIC QUALITY INSPECTED 3

DISTRIBUTION STATEMENT 4
Approved for public release
Distribution Unlimited

Science & Technology

Japan

18th FRP Symposium

JPRS-JST-90-007

CONTENTS

31 January 1990

[Selected papers presented at the 18th FRP Symposium held 15-16 Mar 89 in Osaka]

Agenda [18TH FRP SYMPOSIUM, 15-16 Mar 89]	1
Effect of Water Environment on Propagation of Delamination Fatigue Cracks in CF/PEEK Laminates [Masaki Hojo, Kiyoshi Kenmochi, et al.; 18TH FRP SYMPOSIUM, 15-16 Mar 89]	3
Mode I Fracture Toughness of Tri-Axial 3D Fabric Composites [Nobuaki Mori and Hiroshi Hatta; 18TH FRP SYMPOSIUM, 15-16 Mar 89]	7
Impact Analysis of FRP Rotor Blade [Tokihiko Kawashima, Yasuyuki Tanaka, et al.; 18TH FRP SYMPOSIUM, 15-16 Mar 89]	10

Agenda

43067214A *Osaka 18TH FRP SYMPOSIUM in Japanese 15-16 Mar 89 pp 1-6*

[Text] 1. Maximum Bending Design of Fibrous Laminated Plates Using Lamination Parameters

Department of Aeronautical Engineering, University of Osaka Prefecture, Mitsunori MIKI, Yoshihiko SUGIYAMA and Kenji SAKURAI

2. Object-Oriented Approach for Analysis of Mechanical Behavior of Composites

College of Engineering, University of Osaka Prefecture, Mitsunori MIKI and Yoshihiko SUGIYAMA

3. Development of Personal Computer Program of Stress Analysis for Composite Materials (In case of Isoparametric Elements)

Faculty of Education, Mie University, Masaru ZAKO and Tetsuya TSUJIKAMI

4. Predicted the Failure Strength of Mechanically Fastened FRP Joint

Faculty of Textile Science, Kyoto Institute of Technology, Hiroyuki HAMADA and Zenichiro MAEKAWA

Graduate Student, Kyoto Institute of Technology, Tetsuya TAMURA

5. Reliability Evaluation on Mechanical Characteristics of CFRP

Faculty of Textile Science, Kyoto Institute of Technology, Zenichiro MAEKAWA and Hiroyuki HAMADA

Graduate Student, Kyoto Institute of Technology, Souichi ISHIBASHI

6. Stochastic Materials Design of Composite Materials (Evaluation of Strength of Unidirectional Reinforced Laminate subjected to In-plane Multi-axis Load)

Kanazawa Institute of Technology, Hidetoshi NAKAYASU

SPECIAL LECTURE I

Application of Fracture Mechanics to FRP

Kyoto Institute of Technology, Megumu SUZUKI

7. Effect of Water Environment on Propagation of Delamination Fatigue Cracks in CF/PEEK Laminates

Industrial Products Research Institute, Masaki HOJO and Kiyoshi KEMMOCHI

Department of Engineering Science, Kyoto University, Keisuke TANAKA

LION Corporation, Kazutoshi ENDO

8. Mode I Fracture Toughness of Tri-axial 3D Fabric Composites

Three-D Composites Research Corporation, Akinobu MORI

Mitsubishi Electric Corporation, Hiroshi HATTA

9. FEM Analysis of Dynamic Failure Process of Composite Materials

Department of Naval Architecture, University of Tokyo, Isao KIMPARA

Division of Engineering, Graduate School, University of Tokyo, Kazuo INOUE

Carbon Fiber Project, Toa Nenryo Kogyo, Co., Ltd., Eiki TSUSHIMA

10. Failure Behaviors of Cylindrical Adhesive Joints of GFRP under Combined Loadings (Being Flawed Adhesively Bonded)

Faculty of Engineering, Osaka City University, Katsuhiko OSAKA and Takehito FUKUDA

11. Interactive Effect Between FW Tubes on Lateral Compressive Load

Department of Mechanical Engineering, Doshisha University, Tsuneo HIRAI and Tsutao KATAYAMA

Graduate Student, Doshisha University, Junji HARADA

12. Micro-mechanisms of Failure in Short Glass Fiber Reinforced Thermoplastics 2. - 30w/o and 60w/o SGFR-PET -

Research Institute for Applied Mechanics, Kyushu University, Nak-Sam CHOI and Kiyoshi TAKAHASHI

13. Testing Methods and Results for Acid & Alkali Corrosion of Concrete Sewer Pipe Line with FRP Lining

Himeji Public Works Office of Hyogo Prefecture, Yoshiki URAKAMI

Daicel Technology Service Co., Shojiro TAKASHIMA and Kunio ISHII

14. The influence of Water on Tensile and Fatigue Strength of Angle-Ply Aramid/Epoxy Composites

Department of Mechanical Engineering, Kyoto University, Kenjiro KOMAI, Sohei SHIROSHITA and Sadamu KINOSHITA

Ph. D. Student, Royal Institute of Technology, Sweden, Now Special Course of Kyoto University, J. GRENEDT

15. Water Absorption Anisotropy of Unidirectional CFRP

Government Industrial Research Institute of Osaka,
Yoichiro NAKANISHI and Yoshihiro SAWADA

16. Degradation Behavior of FRTP Laminate, Co-woven
in Consideration of Polymer Orientation Under Hot
Water Environment

Department of Mechanical Engineering, Doshisha Uni-
versity, Tsuneo HIRAI and Tsutao KATAYAMA

Nitto Boseki Co., Ltd., Shimpei ITOH and Hirokazu
INOUCHI

Graduate Student, Doshisha University, Jun ARAKI

17. Flexural Fatigue Tests of FRP Plates Containing
Notches or a Circular Hole

Faculty of Engineering, Fukuoka University, Hiizu
HYAKUTAKE and Terutoshi HAGIO

18. A Method of Fatigue Life Prediction for Composite
Materials

Faculty of Education, Mie University, Masaru ZAKO
and Tetsuya TSUJIKAMI

Toa Nenryo Kogyo Co., Ltd., Yuji ISHIDA and
Hiroyuki YOSHIZAWA

19. Inelastic Behavior of CFRP Under Cyclic Loading

Nagoya University, Yasushi KANAGAWA, Sumio
MURAKAMI and Masahiro NAKAYAMA

Tamagawa University, Yukio SANOMURA

Toa Nenryo Kogyo Co., Ltd., Yuji ISHIDA

20. The Study of Fatigue Failure Mechanism of UD-
CFRP by Means of Surface Replication

Department of Mechanical Engineering, Doshisha Uni-
versity, Sadao AMIJIMA and Toru FUJII

Department of Mechanical Engineering, Kinki Univer-
sity, Takashi MATSUOKA

Graduate Student of Doshisha University, Takeshi
AOKI

21. Temperature Effect on Tensile Fatigue Properties of
GFRP with a Circular Hole

Department of Mechanical Engineering, Doshisha Uni-
versity, Sadao AMIJIMA and Toru FUJII

Department of Mechanical Engineering, Kinki Univer-
sity, Takashi MATSUOKA

Graduate Student, Department of Mechanical Engi-
neering, Doshisha University, Kazuya OHKUBO and
Toshihiro MATSUOKA

22. Fatigue Strength of FRP Bolt Having a Braid Strac-
ture at 293K and 77K

Faculty of Engineering, Osaka University, Yoshihiko
MUKAI and Arata NISHIMURA

SPECIAL LECTURE II

Present Status and Future of Geotextiles

Civil Engineering Materials Sales Department, Mitsui
Petrochemical Industrial Products, Ltd., Nobuo KIY-
OKAWA

23. Visible-light Curing of FRP

Nippon Oil & Fats Co., Ltd., Yoshihiro TOMURA and
Shigeki BANNO

24. Development of Functional Composite Material
Using Metallic Fiber

The Faculty of Engineering, Kobe University, Chiaki
HIWA and Takao NAKAGAWA

Kanai Motor Wheels, Ltd., Akira YOSHIKAWA

25. An Investigation on Testing Method for Tensile
Properties of CFRP

Institute for Medical and Dental Engineering, Tokyo
Medical and Dental University, Hiroo MIYAIRI and
Masahiro NAGAI

26. Research on Flexural Testing Method for Fiber-
Reinforced Plastics

College of Industrial Technology, Nihon University,
Hiroschi IWAI and Masuji UEMURA

Graduate Student of Nihon University, Tohru
HAYASHI

27. On Use of Electric Conductivity for Detecting Flaws
and Fiber Concentrations in CFRP Composites

Department of Aeronautical Engineering, National
Defence Academy, Kazumasa MORIYA and Hiroyuki
HANAWA

28. Evaluation of Impact Damage of Fibrous Composite
Laminates by AE Method (Effect of Fiber Orientations)

Faculty of Engineering, Osaka City University, Takehito
FUKUDA and Katsuhiko OSAKA

Graduate School, Osaka City University, Makoto TAN-
IGUCHI

29. Study on Impact Damage of Laminated Composite
System

Yamagata University, Takashi KURIYAMA, Ikuro
NARISAWA, Atushi SATOU

Tohoku Institute of Technology, Toshihiko ABE

30. Impact Analysis of FRP Rotor Blades

Aero-Engine & Space Operation, Research & Development Department, Ishikawajima-Harima Heavy Industries Co., Ltd., T. KAWASHIMA, T. TANAKA and T. NATSUMURA

31. Promotion for Damping Effect Under Impact Lateral Compression in the Filament-wound Composite with Notch

Department of Mechanical Engineering, Doshisha University, Tsuneo HIRAI, Tsutao KATAYAMA and Nobuyuki KOBAYASHI

32. Hybrid Effects on Impact Behavior of C/A Hybrid Unidirectional FRP Laminates

Graduate School, Kanazawa Institute of Technology, Masayuki NAKADA

Hitachi Research Laboratory, Hitachi Ltd., Shigeo AMAGI

Materials System Research Laboratory, Kanazawa Institute of Technology, Minoru SHIMBO and Yasushi MIYANO

Effect of Water Environment on Propagation of Delamination Fatigue Cracks in CF/PEEK Laminates

43067214B Osaka 18TH FRP SYMPOSIUM in Japanese 15-16 Mar 89 pp 31-34

[Article by Masaki Hojo of the Product Science Laboratories; Kiyoshi Kenmochi of the same laboratories; Keisuke Tanaka of the Engineering Department, Kyoto University; Kazutoshi Endo of Lion Co., Ltd.: "Effect of Water Environment on Propagation of Delamination Fatigue Cracks in CF/PEEK Laminates"]

[Text] CFRP laminates have been applied in primary stage structural material recently and an assessment of its damage tolerance in such actual conditions has grown in importance. The authors have reported in this connection¹ that a CFRP involving a thermoplastic resin PEEK as the matrix, which has been developed recently, displays a notably improved toughness and its laminates have a resistance against delamination fatigue crack propagation which is more than double conventional brittle CFRP laminates of epoxy derivatives. Nevertheless, the resistance of the material against the environmental effects, a property on which much hope has been placed, has so far been scarcely investigated.

This article deals with the mode I delamination fatigue crack propagation behavior to investigate the effects of water environments on CF/PEEK laminates and time dependence of the material, and their relevant mechanisms.

2. Experiment Method

The material used was the APC-2 prepreg laminates of ICI Inc., which the authors had ICI mold into one-way

laminates (0)₄₈ 6 mm in thickness.¹ The specimen was of the double cantilever beam type (DCB) with a width of 20 mm, and a tool with the pin position close to the specimen was used for loading.

2.2 Fatigue Test

The test was carried out with an electric-hydraulic-servo-type testing machine with capacities of 80 N and 9.8 KN connected to a computer under the conditions of a constant stress ratio (ratio of the minimum load to the maximum) and a constant rate of change in the stress intensity factor $(1/K)dK/da$.² The environment for testing chosen was in air at 23°C and 50 percent RH and in water at 23°C and 50°C; the rate of repetition used was 10Hz for the standard and 2 Hz partly for comparison, in load-reduction tests and load-raising tests, respectively. The fatigue test in water was carried out with a trial-manufactured test machine incorporating a horizontal actuator, with the end point of the crack alone dipped in water. The length of the crack was estimated from the compliance characteristics in the course of tests. Here, the relationship between the stress intensity factor K and the energy release rate G was computed using the following formula²

$$K \text{ (MPam}^{1/2}\text{)} = 0.144 \times \text{square root of } G \text{ (N/m)}$$

2.3 Water Absorption Test, Provisionary Processing of Test Specimens in Water Environment

Small pieces excised from the specimen were immersed in water at 23°C and 90°C to investigate their water absorption. Behavior in water absorption at 90°C is shown in Figure 1. The experimental results revealed that the water saturation rate at 0.17 percent was, by a factor of ten, lower than for the CFRPs of epoxy resin, but the rate of diffusion is of the same order, being very slow.³ At room temperature, it takes as long as about 30 years to bring the specimen to the saturation or equilibrium state. In the present experiment, therefore, the test specimen was prepared under the two types of conditions identical with those used for the epoxy-type CFRP to investigate the effects of water.

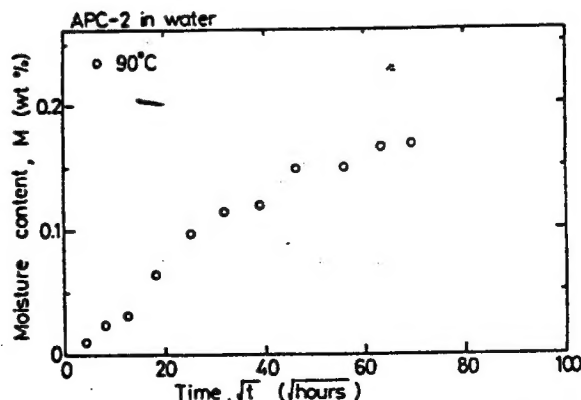


Figure 1. Relation Between Moisture Content and Time

(1) Preliminary Immersion

The specimen was immersed in water for 12 hours without loading before the testing. In this case, water diffuses only over the surface layer of the specimen, but the fracture area at the end point of the crack was so small (30 μm , low-propagation-rate region) that the region contained more than 50 percent of the water required to maintain equilibrium. The preliminary immersion, therefore, conceivably indicates short-term effects of water environments.

(2) Water Control to Reach the Equilibrium

The specimen was subjected to an enhanced water-absorption test in water for some 200 days to reach equilibrium. The specimen underwent no changes in its fracture toughness (K_{IC} of 4.7 $\text{MPa m}^{1/2}$ and G_{IC} of 1270 N) under such a state. The specimen having reached the equilibrium conceivably represents a long-term effect of water environments.

3. Results and Discussions

3.1 Study of the Governing Dynamic Parameters

The authors in their previous report suggested an equivalent stress intensity factor range, ΔK_{eq} , the value of which is given by the following formula, as a parameter that governs crack propagation under different R value conditions, and confirmed that the parameter was applicable also for the case of APC-2.¹

$$\Delta K_{eq} = \Delta K (1 - R)^{\gamma} = \Delta K^{1-\gamma} K_{max}^{\gamma}$$

where γ and $1 - \gamma$ denote the parameters indicating the relative rate at which the maximal load and the repeating load contribute to the propagation [of the crack]. In the present experiment, as previously, γ and hence ΔK_{eq} were computed from the relationship between ΔK and $(1 - R)$ at $da/dN = 10^{-10}$ m/cycle. The value of γ was small—ranging from 0.17 to 0.36—which indicated that the propagation of cracks was largely dictated by the repeating loads.

3.2 Short-Term Effects of Water Environments

The crack propagation rate in water at 23°C and 50°C against ΔK_{eq} for specimens having been previously subjected to the preliminary immersion in water is plotted in Figure 2. The crack-propagation rate is not dependent on the stress ratio, but on the ΔK_{eq} exclusively in the entire relevant range. The behavior of the fatigue crack propagation in water at both 23°C and 50°C differed from that in air (dotted line in the figure) in that there was bending at approximately $da/dN = 5 \times 10^{-10}$ as represented in the exponential relation. The exponential indices varied from 7.1 to 11 and from 6.2 to 18 for water applied at 23°C and 50°C, respectively; in either case, the index was found to be smaller in the low propagation-rate region than in the high. The lower limit

didn't seem to exist under both conditions, and development of time dependence in the low crack-propagation-rate region was conceivable. When compared at the same ΔK_{eq} , the crack propagation rate fell in the region of the higher propagation rate; the differences were a fall to one-third at water temperature of 23°C but to one-half to one-tenth at 50°C. The differences were not notable in the region of low propagation rate. In contrast, 914°C laminates of the epoxy-series had its crack-propagation rate lowered to one-tenth in 23°C water and its exponential index raised enormously in 50°C water. The environmental effects of water on APC-2 laminates were limited in comparison with the above epoxy-laminates, for which one possible reason is that the CFRP using an epoxy resin as the matrix absorbs water up to 2 to 3 percent while APC-2 has a low water absorption of 0.17 percent.

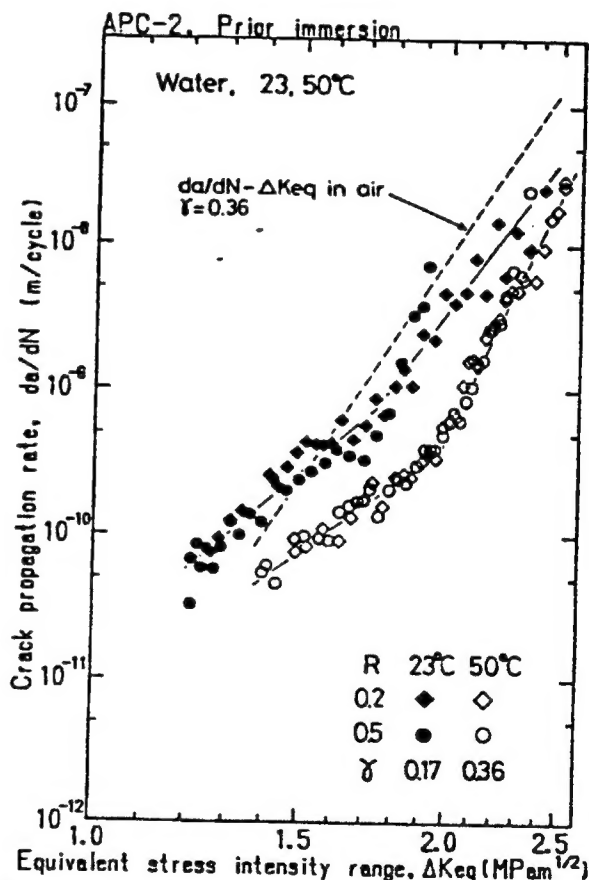


Figure 2. da/dN vs. K_{eq} in Water at 23 and 50°C After Prior Immersion

3.3 Long-Term Effects of Water Environment

Test specimens were immersed in 23°C water where they were subjected to long-term control to reach the saturation limit. Results are shown in Figure 3. For each stress ratio, the curve in the plot indicating an exponential relationship produced bending approximately at da/dN

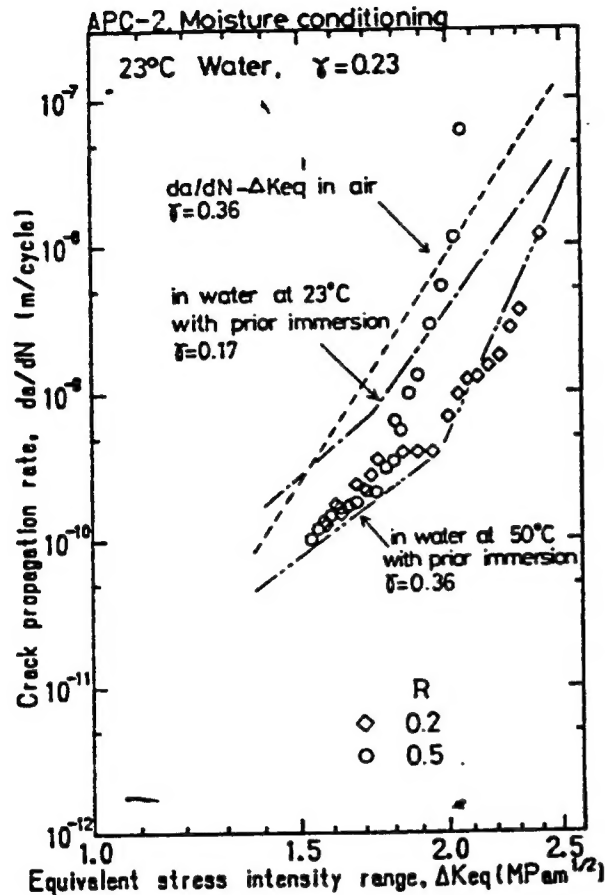


Figure 3. da/dN vs. K_{eq} in Water at 23°C With Moisture Conditioning

$= 5 \times 10^{-10}$ m/cycle, as did the curve for the specimen treated with the preliminary immersion in water, with the exponential index smaller in the region of lower crack propagation rates.

The effects of the stress ratio, in turn, differed between the level above the value of the crack propagation rate da/dN of 5×10^{-10} m/cycle and the one below; the crack propagation rate in the low rate region were dependent on the ΔK_{eq} alone [and independent of the stress-ratio values] while the propagation rate grew with an increase of the stress ratio value in the high-propagation-rate region. For the low-propagation-rate region at R of both 0.2 and 0.5, and for the high-propagation-rate region at $R = 0.2$, the relationship between ΔK_{eq} and da/dN for the specimen subjected to the long-term immersion in water was approximately identical with the one for the specimen subjected to the preliminary immersion followed by the fatigue test at 50°C so that the resistance against the crack propagation for the specimen with the long-term water-immersion was larger than the crack propagation resistance for the specimens subjected to exposure to air alone or to the preliminary immersion followed by the fatigue test at 23°C. index were observed

In the case of the high-crack-propagation-rate region with $R = 0.5$, however, the specimen with long-term water-immersion had a crack propagation rate about five times larger than for those exposed only to air, indicating substantial deterioration in quality. APC-2 has great durability in a normal environment compared to CFRP of the epoxy-series, which, when subjected to the long-term controlled immersion in water, exhibits deterioration in the entire range regardless of the stress-ratio value. For example, the specimen with the long-term immersion in water had a low limit value, 0.65 times than those subjected to the preliminary immersion in water.^{3,4}

3.4 Phenomenon of Time-Dependence

The plot of da/dN vs. ΔK_{eq} representing an exponential relation in Figures 2 and 3 exhibits a knicking of the curve, suggesting a time-dependence developed in the low-propagation-rate region. A 2-Hz load-increasing test, therefore, was carried out in air and in water at 23°C and 50°C, with the preliminary immersion. The result is shown in Figures 4 - 6 adding the results of a relevant 10-Hz experiment in dotted lines for comparison. With results for R of 0.2 alone available, ΔK_{eq} was calculated

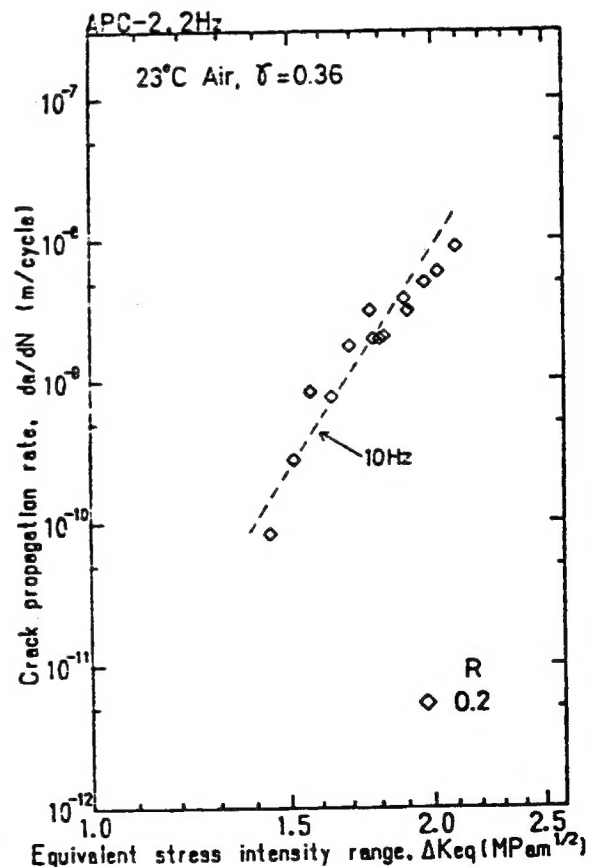


Figure 4. da/dN vs. K_{eq} in Air at 2 Hz

using γ values at 10 Hz. No effects of the rate of repetition was notable in the air as seen in Figure 4, whereas an increase in the crack propagation rate and a fall in the low-propagation-rate region of the exponential in water, with the difference more pronounced in experiments at 50°C, as shown in Figures 5 and 6. In addition, no knicking in the curve for the exponential relationship was notable, the exponential index in the entire crack-propagation-rate region approaching that of the low-crack-propagation-rate region of the 10 Hz curve. A comparison of the rates for 2 Hz and 10 Hz in water at 50°C for the range $\Delta K_{eq} = 1.5 - 2.0 \text{ MPa m}^{1/2}$ proved they differ by a factor of five, equivalent to the difference in the rates of repetition. This implies that the crack propagation in this region is dictated not by repetition, but by time dependence. The knicking seen in the curves of Figures 2 and 3 may conceivably result from the development of time dependence in the low-propagation-rate region.

3.5 Observation of the Fracture Surface

Figure 7 [not reproduced] presents photographs taken with a scanning electron microscope that show fracture surfaces produced in static (fracture-toughness) tests and

in fatigue tests carried out either in air or in water at 23°C, with the specimen subjected to the preliminary immersion or the long-term controlled immersion in water for the fatigue test in water exclusively. In (a), the fracture surface having undergone the static test exhibits a pronounced plastic deformation of the resin and is characterized by an elongation of the resin in the direction normal to the surface: in (b), the fractured surface after the fatigue test in air is rougher indicating that the damage extends deeper toward the inside, but no elongation of the resin is notable. In specimens tested in water at 23°C with the preliminary immersion in water, the fracture surface is similar to the one in (b) for the high-crack-propagation-rate region, but some elongation of the resin, as shown in (c), is notable for the low rate region. For the specimens subjected to the long-term controlled immersion in water, the elongation of the resin is notable in parts for even the high rate-region, and most obvious, as shown in (d), in the low-rate region. Since an elongation of resin more like that for static fracture surfaces was observed in the low-crack-propagation-rate region, the mechanism of the development of this phenomenon may conceivably be closely related to the increased ductility of the resin.

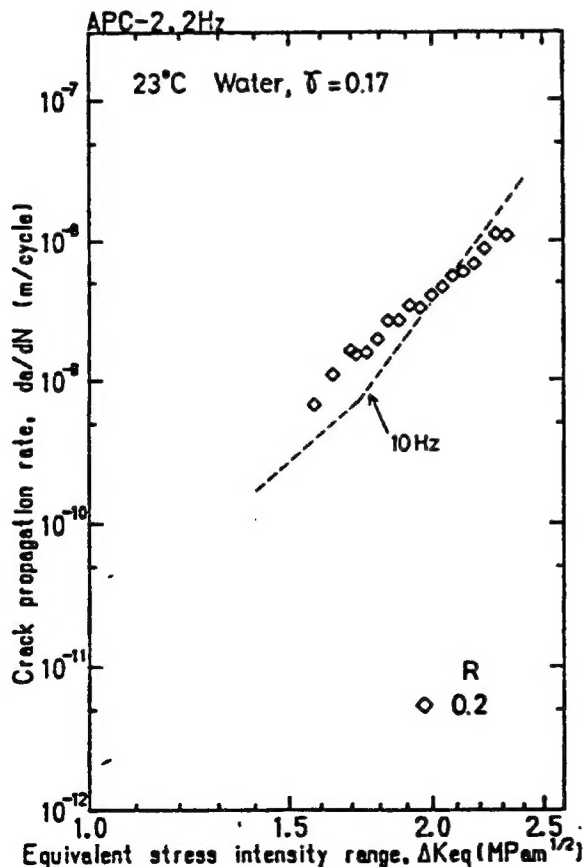


Figure 5. da/dN vs. K_{eq} at 2 Hz in Water at 23°C After Prior Immersion

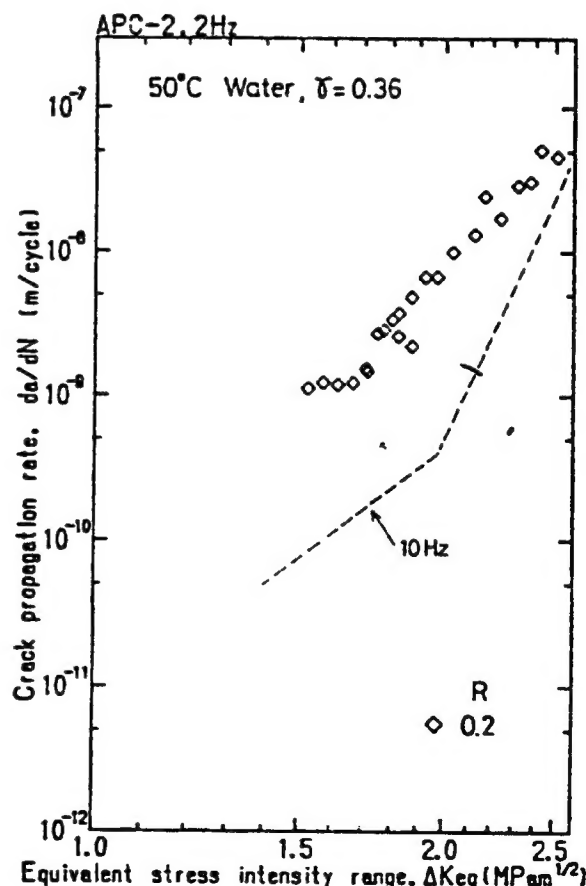


Figure 6. da/dN vs. K_{eq} at 2 Hz in Water at 50°C After Prior Immersion

Numerous reports have been given on the enhancement by water absorption of the creep deformation of polymer materials.

References

1. Masaki Hojo, Keisuke Tanaka, Kiyoshi Kenmochi, Kazutoshi Endo, "Dai-Jusan-Kai Fukugo-Zairyo-Symposium-Koen-Yoshi-Shu" [A Collection of the Abstracts of Lectures at the 13th Symposium on Composite Materials].
2. M. Hojo, K. Tanaka, G. G. Gustafson, and H. Hayashi, *Composite Science Tech.*, (1987) pp 273.
3. Masaki Hojo, Keisuke Tanaka, G. G. Gustafson, Ryuichi Hayashi, "Nippon-Kikaigakkai-Ronbun-Shu" [A Collection of Articles of the Japan Machine Society], 499A, 1988, pp 273.
4. M. Hojo, K. Tanaka, G. G. Gustafson, R. Hayashi, *Proc. ICCM-vi*, Vol 4 (1987) pp 222.
5. For Example: Takeo Yokobori, Ikuo Narusawa, "Kobunshi-Zairyo-Kyodo-Gaku" [The Science on the Strength of Polymer Materials] Baifukan Co. Ltd., 1982, pp 281.

Mode I Fracture Toughness of Tri-Axial 3D Fabric Composites

43067214C Osaka 18TH FRP SYMPOSIUM in Japanese 15-16 Mar 89 pp 35-38

[Article by Nobuaki Mori of 3 D Compo Research Co. and Hiroshi Hatta of Zairyo Kenkyu-Sho [the Material Laboratories], Mitsubishi Electric Co.: "Mode I Fracture Toughness for Three Dimensional Reinforced Composite Materials"]

[Text]

1. Introduction

Three-dimensional fabric-reinforced composite materials (3DCM) may allow the application of advanced composite materials to extend to plastic materials of great thickness and in complicated shapes since it allows laminated composite materials (laminated material) to be designed in a three dimensional form. However, the three-dimensional fabric (3DF), a reinforced 3DCM, involves difficulties in weaving and the effect of three-dimensional arrangement of reinforced fiber on the properties of the fabric has yet to be examined in many points with its basic research.

The present report concerns a 3DCM, using a 3DF with mutually rectangular x, y, and z axes as the reinforcing material, and examines its fracture toughness in comparison with the behavior of laminated materials.

2. Material to Be Tested

Two types of test materials were trial-manufactured; one 3DCM had filaments of 24 Kf with a volume fraction

(Vf) for the fiber of 0.40 and the other, those of 12 Kf with a Vf of 0.49, as shown in Table 1. Laminated materials with filaments 1 Kf and 6 Kf and with Vf in the range of 0.34 to 0.66 were also trial-manufactured for comparison.

Table 1. Raw Material

	Item	3DCM	Laminate
Fiber	Type of fiber	Torayca T300	Torayca T300
	Filaments	6Kfx2 12Kfx2	1Kf 6Kf
Fabric	Vf (total)	0.49 0.40	0.34 - 0.66
	X pitch (mm)	0.92 2.43 (Thk)	1.11 mm 2.5 mm
	Y pitch (mm)	1.05 2.43 (Wld)	1.11 mm 2.5 mm
	Z pitch (mm)	3.60 3.00 (Lng)	
Matrix	Epoxy resins	Bisphenol F diglycidyl ethel	
	Hardener	Methyl hexahydrophthalic anhydride	
	Catalyst	Tridimethyl aminothylphenol	
	Cure temperature	60°C (15h) + 90°C (2h) + 120°C (2h)	

All of these reinforced materials included epoxy resin as shown in Table 1, incorporated by vacuum impregnation for 3DCM and by press molding for the laminated materials. The conditions for hardening for both molding methods were identical. The molded materials of size 300mmX30mmX150mm for 3DCM and 110mmX110mmX11mm for the laminated material were cut to produce the chevron notch test specimens (CN test specimens) for measurement of the work of fracture (W.O.F.) as shown in Figure 1. The laminated material, as seen in Figure 2, was processed into test materials with two different directions of lamination; one flatwise and one edgewise. In carrying out the bending tests, the direction of the maximum density was made to match the lengthwise direction. Table 2 gives mechanical properties measured on these test specimens to compare their static and dynamic destruction behaviors.

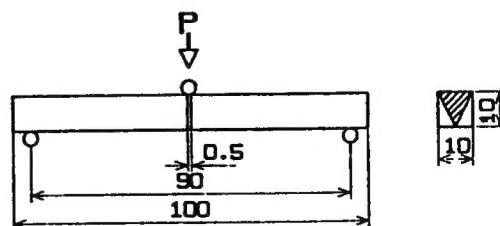


Figure 1. Measurement of W.O.F. With Chevron-Notch Test Specimen

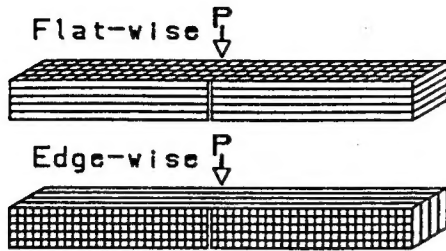


Figure 2. Shapes of the Test Specimens of a Flatwise and Edgewise Laminate

Table 2. Comparison of Properties Other Than Fracture Toughness Between 3DCM and a Laminated Board

Sample	Compressive strength (MPa)	Flexure strength (MPa)	Shear strength (MPa)	Impact energy (J)
3DCM	350	454	162	11.7
Laminate (Flat-wise)	-	323	25	5.9
(Edge-wise)	-	333	80	2.6
(Longitudinal)	228	-	-	-

3. Method of Assessing Fracture Toughness

W.O.F. and the (strain) energy release rate (G_R) were computed from the load-displacement curve obtained by the three-point bending test shown in Figure 1. The measurements were taken with a universal material-testing machine of the Instron corporation, Model 1185, at a crosshead speed of 0.5 mm/min. The CN test-specimen was used because it has special advantages such as its stable growth of cracks eliminating an introduction of initial cracks and that it is suitable for thick materials, hereby providing the assessment of 3DCM with rod-like material.

The W.O.F. represents the amount of work for a unit cross section obtained on the assumption that the total external work applied to the test specimen is consumed in fracture, and calculated by dividing the area singled out by the load-displacement curve and the axis of abscissa in Figure 3 by an area twice that of the projection of fractured surface. Whereas in isotropic material the W.O.F. is equivalent to G_R ,¹ in anisotropic material G_R generally depends on the length of the cracks produced, thus exhibiting the so-called R curve,² and hence some relevant information is necessary in addition to the average value W.O.F. The dependence on crack length of G_R , therefore, was computed from the load-displacement curve by applying Bluhm's slice-model³ and the method of Munz, et al.⁴ The removal and reapplication of loads was repeated in the figure with the view to obtaining the compliance which was necessary for calculating the G_R .

4. Results and Discussion

Results of measurements for W.O.F. are shown in Figures 4(a) and 4(b), which involves flatwise laminated materials and edgewise laminated ones, respectively, for comparison with 3DCM, and wherein the axis of abscissas represents the volume fraction of the fiber arranged lengthwise to the specimen bearing the load. It can be seen from these figures that the flatwise laminated materials has higher W.O.F. values than those edgewise laminated and that the 3DCMs exhibits still higher W.O.F. values. It is also interesting to note that the 6Kf laminated material tends to have larger values than the

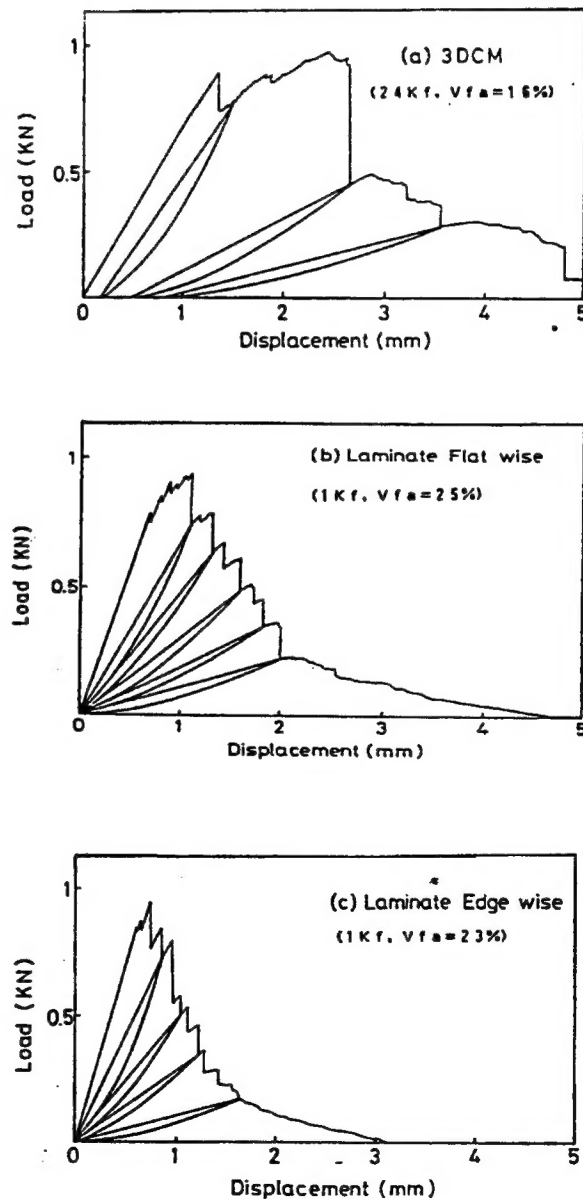
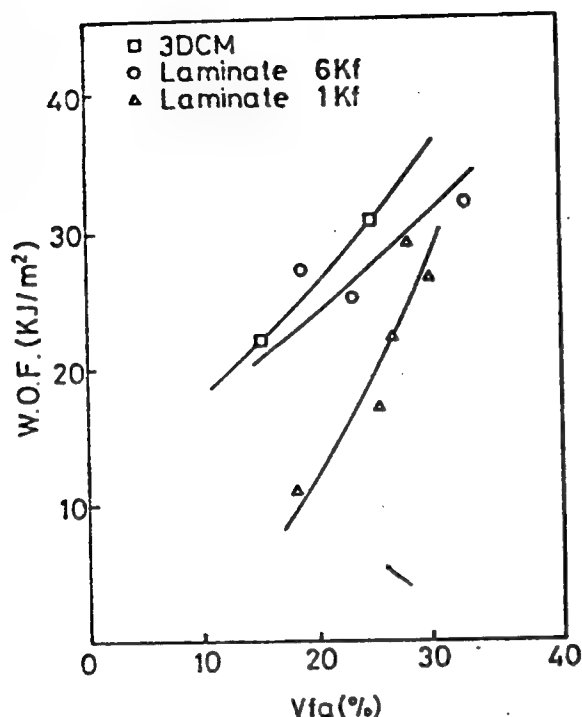
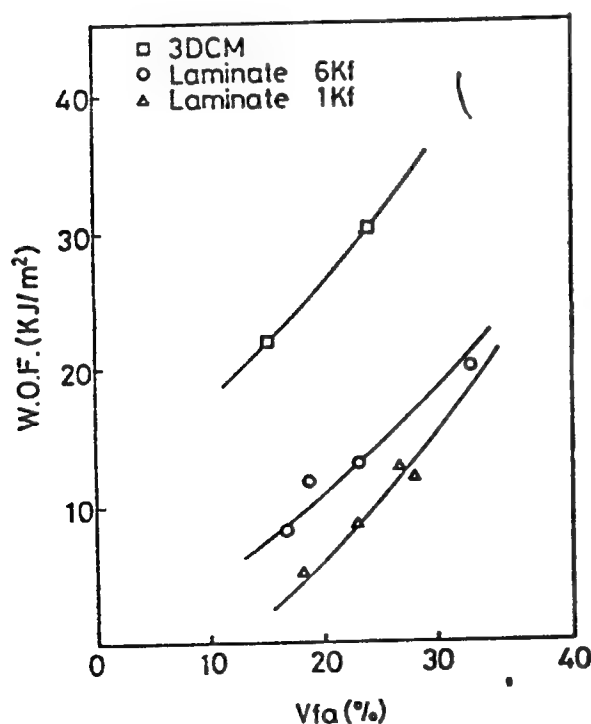


Figure 3. Plot of Stress vs. Strain for Chevron-Notch Specimens



(a)



(b)

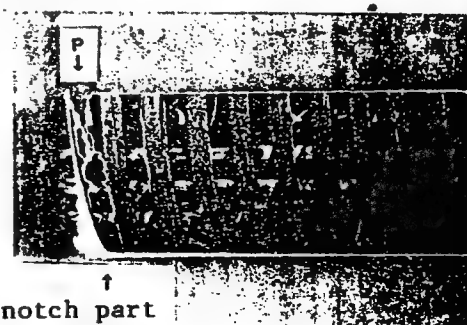
Figure 4. W.O.F. Measurement by a Chevron-Notch Three-Point-Bending Test—(a) Comparison between 3DCM and a flatwise laminate; (b) Comparison between 3DCM and an edgewise laminate

1Kf ones. A notable difference of the fracture process of 3DCM from that of the laminated materials is a separation of composite materials at interfaces between fiber bundles and the matrices accompanied by bridgings generated therein. Figure 5 indicates development of a large number of separations, long ones running normal to the plane of the fractured surface, and those running parallel to the plane at sites slightly apart from the plane. The laminated material lacks these separations totally or, if there are any separations, they are very short.

Whereas the thermal stress developed in laminated materials in the process of their cooling to room temperatures during their molding is released in the direction of layers, the 3DCM has relevant strains built up within because of the effect of the third axis present and resultant stress applied there may conceivably lead to the long-running separation. Development of separation in the interface even by thermal stress alone has been actually observed in some cases where a slightly more brittle resin was used. It is probable that high thermal stress is generated internally even if separation didn't occur.

Such long separation in the bending test may conceivably have resulted from sliding at interfaces between the fiber and the matrix as proved by the fact that, of the three curves of deloading or decreasing loads in Figure 3, the one for 3DCM alone does not return to the zero-load level, retaining a permanent deformation. At the advancing front of the crack, at this juncture, a bridging of the crack with fiber bundles as shown in Figure 6 occurs. As investigated and reported on composite materials with brittle matrices, bridging with fiber bundles acts to block the crack-opening displacement (COD), which provides a highly probable mechanism for the toughness of composite materials.² Since the bridging effect is more notable as the interface separation grows larger, though relevant quantitative estimation has yet to be carried out, the mechanism seems to explain in detail the experimental results for the toughness of 3DCM.

Bridging of fiber bundle doesn't possibly occur in the absence of cracks; the bridging manifests its effect as the crack advances. Figure 7 shows the R curve effect



Chevron-notch part
(fracture surface)

Figure 5. Damages Produced by W.O.F.-Test for 3DCM

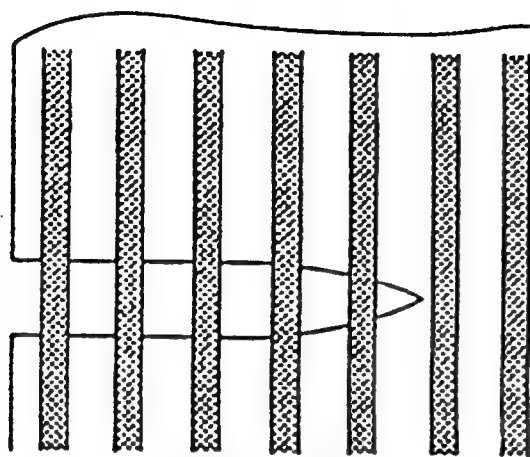
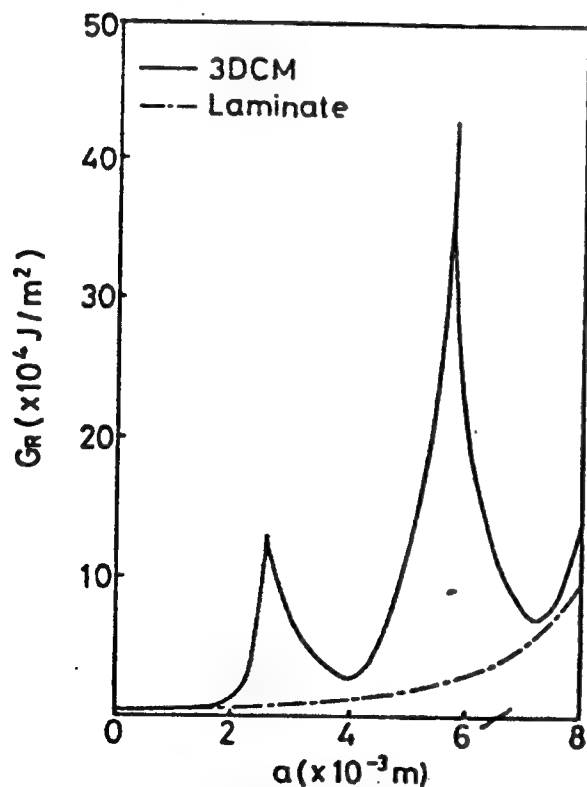


Figure 6. Model for Bridging by Fibers

Figure 7. Plot of Strain-Energy-Release-Rate, G_R , vs. Crack Length

involved, with the axis of ordinate representing G_R and the axis of abscissa, the length of cracks a , as estimated by compliance.

Though there remains some room for dispute in the direct application of the method of linear fracture

dynamic for isotropic materials, only in the case of 3DCM, can cyclic increase and reduction of the G_R by bridging and fiber breakdown be observed clearly. The interval between the G_R peaks presents a similar value similar to the configuration of fiber bundles, therefore the energy created through fracture is absorbed in each layer in large quantity.

The great toughness of the 3DCM discussed above is also proved by the impact [energy] value listed in Table 2 with the material showing energy absorption in larger quantity when compared to the laminated materials. It also shows a fracture pattern similar to that of the chevron test specimen, which will henceforth be investigated further.

References

1. Toshihiko Nishida and Eiichi Yasuda (compiling), "Ceramics no Rikigakuteki Hyouka [Dynamic Assessment of Ceramics]" Nikkan kougyou Shinbun Co., 1986, pp 97-124.
2. Budiansky, et al., J. Mech. Phys. Solids, 34, pp 167-189 (1986).
3. Bluhm, J. I., Eng. Fracture Mech., 7, pp 593-604 (1975).
4. Munz, D., et al., J. Ame. Ceram. Soc., 63, p 300-305 (1980).

Impact Analysis of FRP Rotor Blade

43067214D Osaka 18TH FRP SYMPOSIUM in Japanese 15-16 Mar 89 pp 129-132

[Article by Tokihiro Kawashima, Yasuyuki Tanaka, and Tadashi Natsumura: "Impact Analysis of FRP Rotor Blade"]

[Text]

1. Introduction

Composite materials made by laminating unidirectional materials are favored over ordinary metals in specific rigidity and specific strength and, in recent years, have begun to be used aggressively as components for jet engines of aeroplanes. Some practical applications in static components have been already seen. In the practical application of FRP in a rotational component, e.g., a rotor blade, however, the damage produced to the component by colliding ice, stones, birds, etc. at high speeds (Foreign Object Damage: FOD) poses a serious problem. This report deals with a basic experiment and analysis for impact responses by use of a cantilever board as the model of the blade in order to assess the damages produced in cases where impact is applied to the FRP blade at high speeds.

2. Impact Experiment

2.1 The Method of Experiment

A diagram of the test apparatus is presented in Figure 1. A steel ball (ϕ 5 mm, 0.5 gm) was used for the projectile

for collision with the object to be tested. The steel ball was accelerated with gun powder to a speed of 100 - 500 meters per second and made to collide with a stationary test object. The speed of the steel ball at collision was

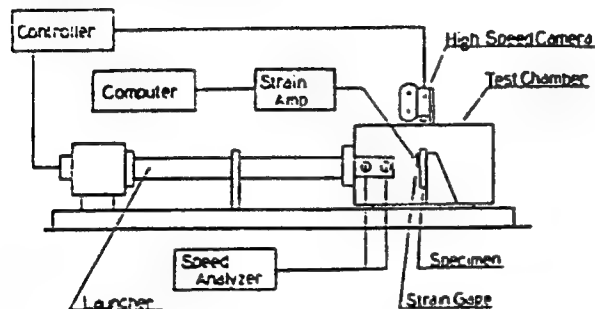


Figure 1. Block Diagram of the Apparatus

under control by adjusting the amount of the gun powder based on some preliminary testings. The data obtained by measurements are for speeds of the projectile at the time of collision and strain responses at the time of collision registered by a strain gage applied to the test object. The process of deformation was recorded with a high speed camera.

2.2 The Object To Be Tested

The test object used was a hybrid laminated board combining glass (G) and Kevlar (K). The type of lamination was plain weaving (UD). The structure of the lamination and results of the three-point bending test for strength are shown in Table 1. The test object, as a simplified model for the blade, was a flat board rectangular in shape and fastened in a cantilever state using relevant tools. The shape of the test piece and the sites at which the projectile collided and at which the strain gages were applied are shown in Figure 2.

Table 1. Laminates

Type of laminate	A	B	C	Data for the bending test				A: 0/90/0
				0° Rigidity	90° Rigidity	0° Strength	90° Strength	B: 90/0/90
G/K UD	G	K	K	2743	2446	87.3	66.2	C: 0/90/0/90
								Volume of laminates ABABCBA

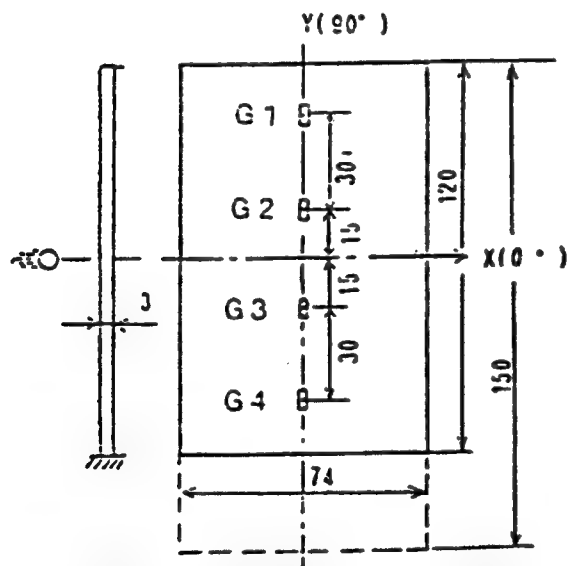


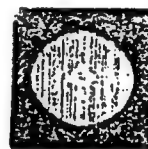
Figure 2. Simplified Model of the Blade

2.3 Results of the Experiments

The strain responses and the damage mode produced at the site of collision by a high-speed collision test will follow.

(1) Damage Mode

The mode of the damage produced at the time of collision for the FRP flat board is shown in Figure 3,



(a) Cloth material (b) UD material

Figure 3. Damage Mode (opposite surface)

along with that for cloth material carried out simultaneously. The speed of the projectile at the time of collision was 140 meters per second, a value below the limit of penetration. As can be seen from the figure, a wide-ranged separation of laminated layers was produced in a concentric area surrounding the site of collision in the case of cloth material and in the direction determined by the orientation of the fiber in the case of the UD material.

(2) Dynamic Strain Response

Figure 4 shows strain responses measured at sites G3 and G4 at the time of collision with the strain gages applied to the test object at these sites to make measurements. The interval between the adjoining data sampling times was 20 μ second for Figure 4 (a) and 0.2 μ second for Figure 4 (b). It can be seen from Figure 4 (a) that, after a perturbation just after the collision of the projectile, the wave turns into a sine wave gradually. Natural periods

with frequencies of some 130 HZ and 830 HZ are also observed in G3-waves which represent the frequencies of primary and secondary bendings, respectively. In Figure 4 (b), in turn, is displayed the wave on an expanded scale for 200 μ second after the collision. Differences in time for the point of the beginning of the rise of the wave and for that of the maximum wave amplitude are notable between sites G3 and G4. For the distance of the applied gages of 30 mm, the speeds of propagation of the waves are computed to be 5000 meters per second and 520 meters per second, and the former value compares with the elastic-wave propagation speed where the value for

$$(\sqrt{E/P} \approx 4 \\ 000 \text{ m/s})$$

Young's modulus in Table 1 is used for calculation, whereas the latter value may possibly represent the speed of the propagation of the wave for the bending of the board.

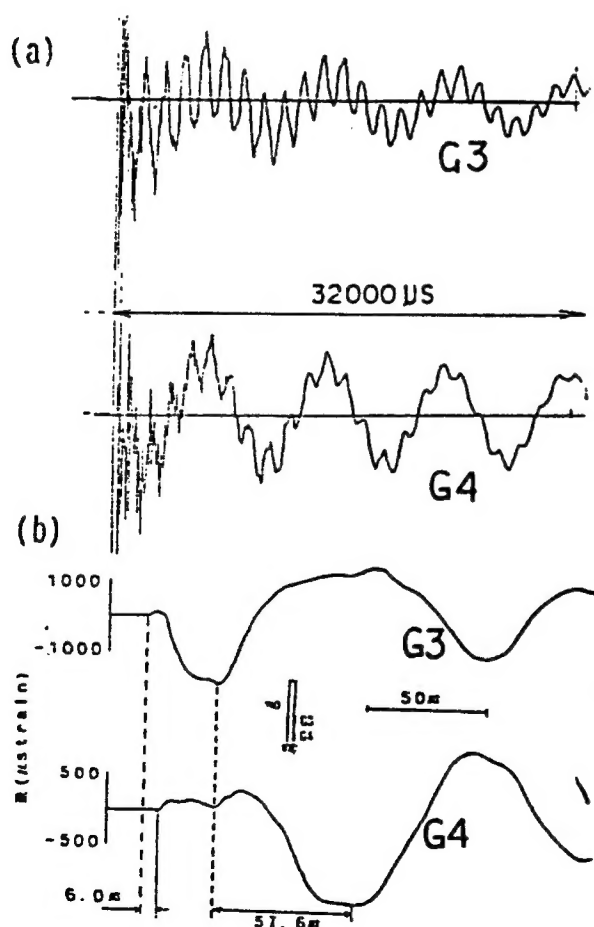


Figure 4. Strain Response to Impact (experiment)

3. Analysis of Impact Responses

It is possible to reproduce and assess the damage mode providing the impact of loading and the contact time of the projectile with the test object at the time of impact, among other things, are clarified and representation of the impact response waves obtained in experiments by a proper form in analysis is possible. An analysis for impact responses using the finite element method, therefore, was carried out, where a simplified blade model was used and results compared with those of the above experiments.

3.1 The Method of Analysis

The general-purpose FEM-program, MSC/NASTRAN, and MARC were used for the analysis. Material parameters in Table 2 were used as the shell elements suitable to the analysis of laminated structures.

Table 2.		
Property	Lamina type	
	G	K
E 1	4000	7500
E 2	900	600
G 12	400	400
v 12	0.26	0.34

Before starting the impact analysis, analyses on the natural frequencies of the blade model and on relevant static loading were carried out and results obtained were compared with relevant experimental ones (Table 3: natural frequency; Figure 5: static analysis) with the view to confirming the correctness of applying the above programs and the parameters. Relevant analyses corresponded well with experimental results and sufficient precision was probable for response analysis. There are three types available for the input in the response analysis as shown in Figure 6: (a) The time related shape of the impact loading, (b) the initial velocity, (c) the projectile (concentrated mass and its velocity). The (a) method was the one adopted here.

Table 3.				
	Mode	1 (HZ)	2	3
Experiment		133.5	345	835
Analysis	MARC	133.0	343	836
	NASTRAN	136.0	391	853

3.2 Results of Analysis for Impact Responses

In connection with low-speed impacts, an analysis was made in cases where impacts were given to the blade model with an impact hammer incorporating a load cell at its head. The shape of the input wave, values of the loads, and contact time required for the load input had been all provided by relevant experiments. Under this condition the analysis was made and the test results were

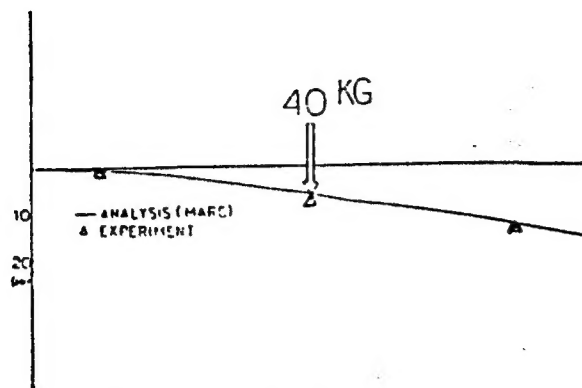


Figure 5. Static-Load Analysis (MARC)

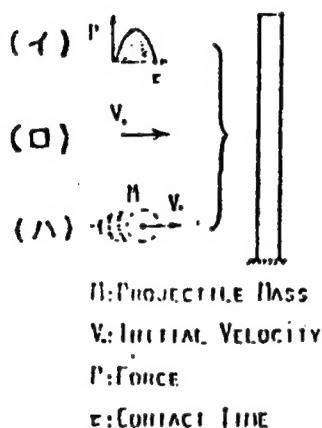


Figure 6. Method of Input for Impact Analysis

confirmed to be same as that of response wave-forms. (The results are omitted.) As for such experiments like this which involve high-speed impact, however, it was hard to measure impact conditions. Hence the value of maximum impact load, one of the input parameters, had to be hypothesized as fixed. Then by varying wave shape and contact time, conditions best adapted to the actual wave were derived. Changes of transient responses to input data are presented in Figure 7. Final results of analysis and those of experiments for the transition of strain responses in the direction of the span are shown in Figure 8, and show good agreement as far as the range (within 200 μ s) just following the impact is concerned. In particular, the time difference when the strain wave starts to rise and the time difference of maximum amplitude between sites G3 and G4 are 4300 meters per second and 570 meters per second respectively. These figures with those values were obtained by the experiments. The sine wave, as an input wave, thus proved with certainty to be capable of producing response waves properly and the contact time to affect the simulation results in a large measure. It was also proved that the impact load affects the amplitude of the [response] wave. General-purpose programs, meanwhile, often offer a procedure for impact analysis wherein a projectile or

Wave Shape of the Input TRANSIENT RESPONSE (G3)

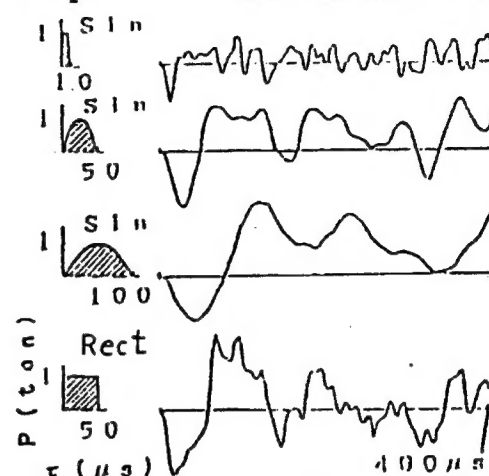


Figure 7. Change in Response With Time-Related Load Patterns (NASTRAN)

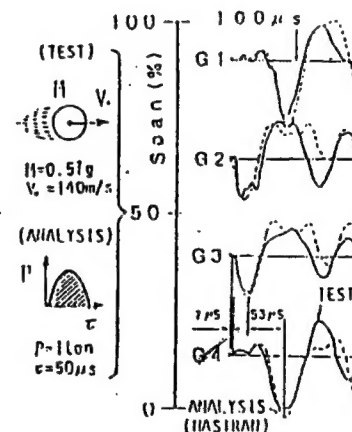


Figure 8. Transitional Process of Strain Response to the Impact

concentrated mass provided with an initial velocity is collided with the test object. This method, which is convenient enough to allow direct computation of contact times, impact loads, etc., was used in the present analysis for the estimation of the value of the impact load for reference sake.

In Figure 9 are shown the deformation modes in the present analysis. It can be seen that a localized deformation propagates from the center, the impact point, toward the periphery, with the mode shifting from the primary bending to the secondary. It was reported that, for a flat board fastened on all four sides, the speed of propagation of the maximum strain-amplitude agreed

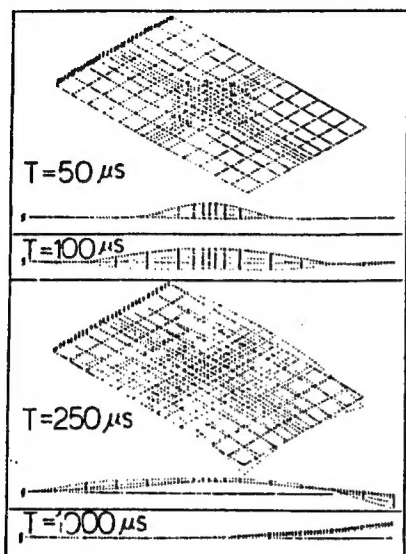


Figure 9. Deformation Mode Upon Impact

with the speed of the progress of the separation of the laminated layers measured with the relevant high-speed photographs.

3.3 Assessment of Damage

A final assessment of the damages must be made following the procedures so far given above. Since composite materials show a wide variation in strength, it seems difficult to establish criteria for the quantitative assessment of the damages before more data is accumulated. In the present analysis, therefore, a qualitative assessment was tried with inter-layer shear stress and Hoffmans' destruction-rule formula; Figure 10 shows a distribution of parameters for each of interlayer shear stress and Hoffman in a cross-section at the point of the impact. The parameters for interlayer shear stresses grow at the center of lamination and those of Hoffman on the back side of the board and particularly the fact that the damage is greater on the back side rather than the front in the distribution of Hoffman agrees with the actual damage. It is henceforth necessary to verify various destruction rules and to clarify the mechanism of inter-layers separation along with accumulation of data in large numbers.

4. Conclusion

A parametrical analysis of experiments was conducted on a model blade with the view to assessing the blade made of FRP, with the following results.

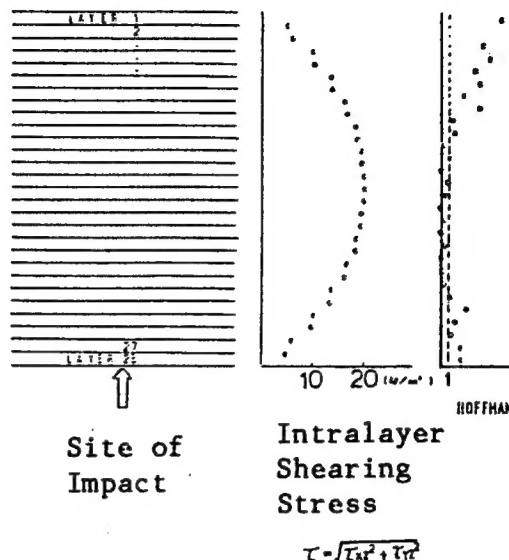


Figure 10. Degrees of Damage at the Site of Impact

(1) An impact test on a blade model was conducted and behavior of the blade assessed for the period immediately following the impact and for a span that follows that period.

(2) An impact analysis was made on the basis of the impact strain-responses measured in order to optimize the load for the impact and it has been proved with certainty that a general-purpose FEM program allows simulation analysis of composite materials.

(3) The relevant parameters distributed on the basis of Hoffman's destruction rule proved that the result agreed with relevant experimental results qualitatively.

References

1. Takeda, NIPPON FUKUGO-ZAIRYO KAGAKU-KAI-SHI [Journal of Japan Composite Material Science Society], 12, 2 (1986).
2. C. C. Chamis and M. D. Minich Ashe 75-GT-78.
3. Aono, Kawashima, Nakamaru, "The 14th FRP Symposium" 5, 1985.
4. Takeda, "Dai-Nijugo-kai Hikoki Symposium" [The 25th Aeroplane Symposium].
5. MARC ADVANCE COURSE ON METAL FORMING ANALYSIS AND VISCO-ELASTICITY (1987).

10
22161

45

NTIS

ATTN: PROCESS 103

5285 PORT ROYAL RD

SPRINGFIELD, VA

22161

This is a U.S. Government publication. Its contents in no way represent the policies, views, or attitudes of the U.S. Government. Users of this publication may cite FBIS or JPRS provided they do so in a manner clearly identifying them as the secondary source.

Foreign Broadcast Information Service (FBIS) and Joint Publications Research Service (JPRS) publications contain political, economic, military, and sociological news, commentary, and other information, as well as scientific and technical data and reports. All information has been obtained from foreign radio and television broadcasts, news agency transmissions, newspapers, books, and periodicals. Items generally are processed from the first or best available source; it should not be inferred that they have been disseminated only in the medium, in the language, or to the area indicated. Items from foreign language sources are translated; those from English-language sources are transcribed, with personal and place names rendered in accordance with FBIS transliteration style.

Headlines, editorial reports, and material enclosed in brackets [] are supplied by FBIS/JPRS. Processing indicators such as [Text] or [Excerpts] in the first line of each item indicate how the information was processed from the original. Unfamiliar names rendered phonetically are enclosed in parentheses. Words or names preceded by a question mark and enclosed in parentheses were not clear from the original source but have been supplied as appropriate to the context. Other unattributed parenthetical notes within the body of an item originate with the source. Times within items are as given by the source. Passages in boldface or italics are as published.

SUBSCRIPTION/PROCUREMENT INFORMATION

The FBIS DAILY REPORT contains current news and information and is published Monday through Friday in eight volumes: China, East Europe, Soviet Union, East Asia, Near East & South Asia, Sub-Saharan Africa, Latin America, and West Europe. Supplements to the DAILY REPORTs may also be available periodically and will be distributed to regular DAILY REPORT subscribers. JPRS publications, which include approximately 50 regional, worldwide, and topical reports, generally contain less time-sensitive information and are published periodically.

Current DAILY REPORTs and JPRS publications are listed in *Government Reports Announcements* issued semimonthly by the National Technical Information Service (NTIS), 5285 Port Royal Road, Springfield, Virginia 22161 and the *Monthly Catalog of U.S. Government Publications* issued by the Superintendent of Documents, U.S. Government Printing Office, Washington, D.C. 20402.

The public may subscribe to either hardcover or microfiche versions of the DAILY REPORTs and JPRS publications through NTIS at the above address or by calling (703) 487-4630. Subscription rates will be

provided by NTIS upon request. Subscriptions are available outside the United States from NTIS or appointed foreign dealers. New subscribers should expect a 30-day delay in receipt of the first issue.

U.S. Government offices may obtain subscriptions to the DAILY REPORTs or JPRS publications (hardcover or microfiche) at no charge through their sponsoring organizations. For additional information or assistance, call FBIS, (202) 338-6735, or write to P.O. Box 2604, Washington, D.C. 20013. Department of Defense consumers are required to submit requests through appropriate command validation channels to DIA, RTS-2C, Washington, D.C. 20301. (Telephone: (202) 373-3771, Autovon: 243-3771.)

Back issues or single copies of the DAILY REPORTs and JPRS publications are not available. Both the DAILY REPORTs and the JPRS publications are on file for public reference at the Library of Congress and at many Federal Depository Libraries. Reference copies may also be seen at many public and university libraries throughout the United States.